Mechanics and Mechanical Engineering
Vol. 17, No. 3 (2013) 235–249
© Lodz University of Technology

Application of Photoelasticy for Study of Lamellar Cracks

Mieczysław Jaroniek
Department of Strength of Materials
Łódź University of Technology
Stefanowskiego 1/15, 90–924 Łódź, Poland

Tadeusz Niezgodziński
Department of Dynamics
Łódź University of Technology
Stefanowskiego 1/15, 90–924 Łódź, Poland

Received (10 March 2013)
Revised (16 May 2013)
Accepted (20 July 2013)

In rolled sheets, non–metallic inclusions are distributed along the thickness of the sheet as narrow lines running parallel to the rolling direction. Such inclusions are the nuclei of lamellar cracks.

This work presents the application of the photoelastic method for study of lamellar cracking. Photoelastic models of samples with long artificial fissures set in the area of the sheet axis were studied along with other encountered inclusion distributions.

The studied samples were placed in a polariscope and subjected to uniform tension; isochromatic images were obtained. Changes in the stress state in the area of the inclusion were observed as the load increased. Stress concentration leads to the formation of lamellar cracks – the joining of voids in the direction parallel to the exterior surface of the sheet (so–called "terraces" are formed) and at angles (so–called "jogs" are formed).

The results of photoelastic tests were compared with the results of numerical calculations using the finite element method.

Keywords: Non–metallic inclusions, photoelastic tests, finite element method, lamellar cracking

1. Introduction

Was performed of experimental analysis of stress and deformation of steel elements with lamellar cracks. These cracks are formed in the rolled sheets containing non–metallic inclusions. In cases where the existence of cracks in the vicinity of the vertex under the influence of external loads created stress concentrations.

During the load components of stress and strain measurements around cracks is impossible.

Photographs of scanning electron microscopy can be obtained before and after the destruction of the load. However, the use of scanning electron microscopy in combination with the testing machine is impossible.

If such stress concentration indirect methods can be used such as by shaping a similar structure photoelastic method, and then on the basis of the numerical models of experimental form.

For experimental studies were made of similar construction models as samples cut from sheet steel with lamellar cracks. System structure model based on photographs obtained with a scanning electron microscope. The study was conducted using the photoelastic method. Models were prepared from optically active polymer materials.

The photoelastic method can also be used to validate a numerical model based on the finite element method.

This work presents the application of the photoelastic method to the study of lamellar cracking.

In the case of adhesion between the base material and non–metallic inclusions, changes of the stress state are observed along the direction of tension between inclusions as well as in the vicinity of inclusions. Changes in stress distribution occur here, which may cause an increase in shear stress along the lines connecting the vertices of inclusions. According to hypotheses concerning strain analysis in an elastic–plastic state, this can have an effect on the formation of cracks. Non–metallic inclusions have a significantly lower strength and elasticity (Young's modulus) than (in this case) ferritic–pearlitic steel. Such inclusions may have the nature of voids and can become crack nuclei. Fig. 1 shows a typical ferritic–pearlitic steel structure with banding encountered after single–direction rolling. Non-metallic inclusions of manganese sulfides can be seen in the cross–section.

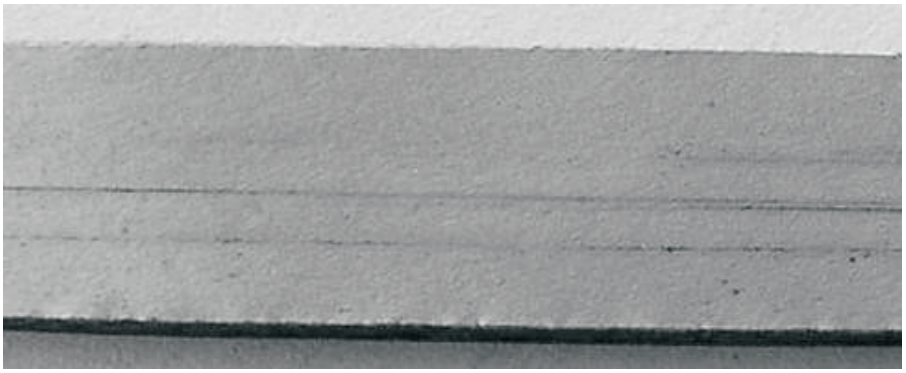

Figure 1 Metallographic specimen of a sheet with visible inclusions

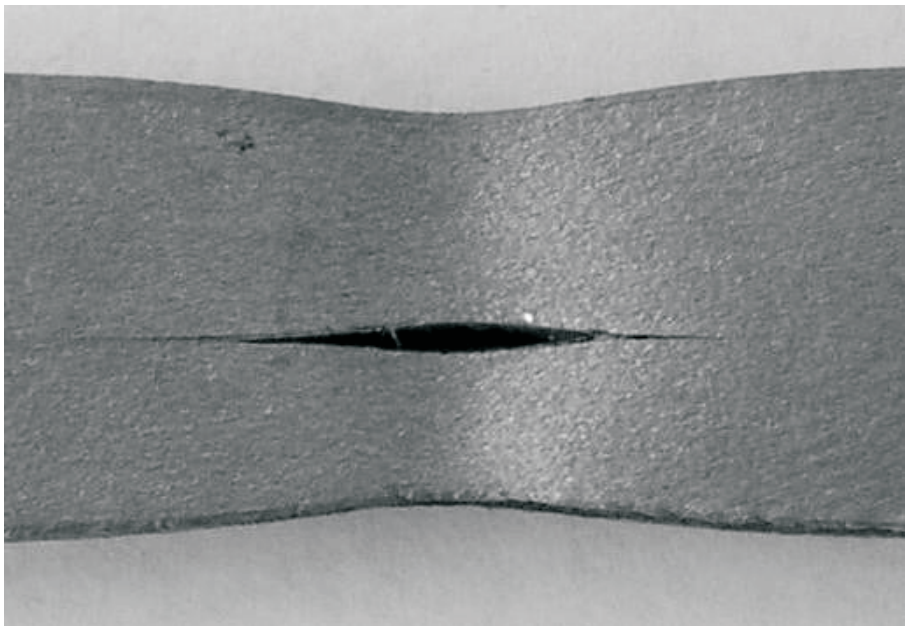

Figure 2 View of the sample just before tearing

During static tensile testing of such samples, an increase in the thickness of the fissure with non–metallic inclusions and the appearance of two characteristic "necks" can be observed.

Non–metallic inclusions are the nuclei of the formation of lamellar cracks. Photoelastic models of samples with long artificial fissures set in the area of the sheet axis were studied along with other encountered inclusion distributions.

2. Methods of stress measurement using the photoelastic method

General procedures for photoelastic measurements have been presented in many text books [1, 2, 3]. Principal stresses σ_1, σ_2, σ_3 are the primary quantities for determining the load-bearing capacity of an element or structure (in the case of a coplanar stress state $\sigma_1 > \sigma_2$, $\sigma_3 = 0$). For given stress component data in a Cartesian coordinate system (σ_x, σ_y and τ_{xy}), principal stresses are usually calculated on the basis of elementary formulas used in strength of materials. The distribution of isochromatic lines makes it possible to evaluate the stress state according to the maximum shear stress hypothesis

$$2\tau_{\max} = \sigma_1 - \sigma_2 \tag{1}$$

and to immediately determine areas of stress concentration in the entire area of the model. Studies and calculations were conducted for beams that were bent on both sides, so that the results (stress distributions) could be applied to fatigue calculations.

The stress distribution in was determined using two methods: **Shear Stress Difference Procedure** (SDP – evaluation a complete stress state by means the isochromatics and the angles of the isoclines along the cuts) [3] and **Method of the characteristics** (the stress distribution were determined using the isochromatics only and the equations of equilibrium [8].

2.1. *Shear stress difference procedure (SDP)*

Using internal equilibrium differential equations (for a coplanar stress state) and the results of photoelastic measurements, the components of stresses σ_x, σ_y, τ_{xy} along any linear cross-section of the model can be determined. Based on photoelastic measurements for a given point, the difference between principal stresses can be determined

$$\sigma_1 - \sigma_2 = k_\delta m \tag{2}$$

along with the isoclinic line. The shear stress value is determined by the formula

$$\tau_{xy} = \frac{\sigma_1 - \sigma_2}{2} \sin 2\alpha = \frac{1}{2} k_\delta m \sin 2\alpha \tag{3}$$

and the difference between normal stresses

$$\sigma_x - \sigma_y = (\sigma_1 - \sigma_2) \cos 2\alpha = k_\delta m \cos 2\alpha \tag{4}$$

The shear–difference method is based on approximated integration of internal equilibrium equations of a plane stress state

$$\begin{cases} \frac{\partial \sigma_x}{\partial x} + \frac{\tau_{xy}}{\partial y} = 0 \\ \frac{\partial \sigma_y}{\partial y} + \frac{\tau_{xy}}{\partial x} = 0 \end{cases} \tag{5}$$

By means the angles of the isoclinics the isochromatics along the cuts "y" et "y+Δy" by the aid of SDP it is possible determined a complete stress state.

$$\sigma_{xi} = \sigma_{xo} - \sum_1^i \Delta\tau_{xyi} \frac{\Delta x}{\Delta y} \tag{6}$$

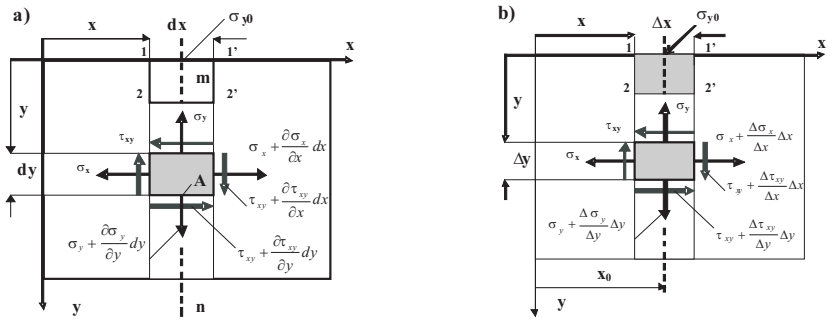

Figure 3 Components of the differential stress (a) as well as finite differences (b)

Distribution of stresses acting on the element structure where:

σ_{yo} – stress–free boundaries

$\Delta\tau_{xyi} = \tau_{xyi}(y + \Delta y) - \tau_{xyi}(y)$ – shear stress difference

$\tau_{xyi}(y+\Delta y)$, $\tau_{xyi}(y)$ – shear stresses in points **i** et **i'** respectivelly in cuts "y+Δy" and "y"

$$\tau_{xy}(y)_i = \tfrac{1}{2}(\sigma_1 - \sigma_2)_i \sin 2\alpha_i = \tfrac{1}{2} k_\sigma m_i \sin 2\alpha_i \tag{7}$$

$k_\sigma m_i = \sigma_1 - \sigma_2$ – the principal stress difference

$k_\sigma = (f_\sigma)_{1.0}/b$ – photoelastic constant

m_i – the order of isochromatic

α_i – the angle of isoclinic (between x and σ_x if $\sigma_x > \sigma_y$)

The distribution of the stresses alog the x - axis were determined from:

$$\begin{array}{l} \sigma_{yi} = \sigma_{xi} - (\sigma_1 - \sigma_2)\cos 2\alpha \\ \tau_{xy}^m = \frac{1}{2}[\tau_{xy}(y + \Delta y)_i - \tau_{xy}(y)_{i'}] \end{array} \tag{8}$$

The details of this method have been given in works [1, 2], among others.

2.2. *Method of characteristics*

The method allows to determine the characteristics of the stress distribution on the basis of image the isochromatics. We assume that the principal stress directions and the sum of the principal stresses are certain functions. We assume that these functions are known. Knowing their differentials and taking into account the balance equations we obtain a system of equations. After solving the system of equations along the characteristics of the components of the stress get.

Because the units are operating photoelastic measurements of the isochromatics rows and practice the stress of the final results obtained in units multiplied by a photoelastic constant k_σ of the model to simplify the method presented in the following discussion taken $k_\sigma = 1$.

Thus, the sum and difference of principal stresses can be written as follows:

$$\left\{ \begin{array}{l} \sigma_1 - \sigma_2 = m \\ \sigma_1 + \sigma_2 = 2p = q \end{array} \right. \tag{9}$$

Assuming that functions and $p$are known, stress components are substituted into the system of equilibrium equations:

$$\left\{ \begin{array}{l} \sigma_x = p + \frac{m}{2}\cos 2\varphi \\ \sigma_y = p - \frac{m}{2}\cos 2\varphi \\ \tau_{xy} = \frac{m}{2}\sin 2\varphi \end{array} \right. \qquad \left\{ \begin{array}{l} dp = \frac{\partial p}{\partial x}dx + \frac{\partial p}{\partial y}dy \\ d\varphi = \frac{\partial \varphi}{\partial x}dx + \frac{\partial \varphi}{\partial y}dy \end{array} \right. \tag{10}$$

The derivatives of the unknowns of functions and p are complete differentials. Considering the complete differentials of functions φ and p, and assuming that these functions are known, a system of four linear algebraic equations is obtained in view of

$$\frac{\partial p}{\partial x}, \quad \frac{\partial p}{\partial y}, \quad \frac{\partial \varphi}{\partial x}, \quad \frac{\partial \varphi}{\partial y}$$

the system of equations takes the form:

$$\begin{cases} \frac{\partial p}{\partial x} - m\sin 2\varphi\frac{\partial \varphi}{\partial x} + m\cos 2\varphi\frac{\partial \varphi}{\partial y} = -\frac{1}{2}\left(\frac{\partial m}{\partial x}\cos 2\varphi + \frac{\partial m}{\partial y}\sin 2\varphi\right) \\ \frac{\partial p}{\partial y} + m\cos 2\varphi\frac{\partial \varphi}{\partial x} + m\sin 2\varphi\frac{\partial \varphi}{\partial y} = -\frac{1}{2}\left(\frac{\partial m}{\partial x}\sin 2\varphi - \frac{\partial m}{\partial y}\cos 2\varphi\right) \\ \frac{\partial p}{\partial x}dx + \frac{\partial p}{\partial y}dy = dp \\ \frac{\partial \varphi}{\partial x}dx + \frac{\partial \varphi}{\partial y}dy = d\varphi \end{cases} \tag{11}$$

If the characteristic determinant of the system (11) is equal to zero, then functions φ and $p$are not unique and the above system of equations has an infinite number ofsolutions.

The "L" curves along which functions and p are assumed are called the characteristics of a system of differential equations; the determinant of the system can be written as follows:

$$\begin{vmatrix} 1 & 0 & -m\sin 2\varphi & m\cos 2\varphi \\ 0 & 1 & m\cos 2\varphi & m\sin 2\varphi \\ dx & dy & 0 & 0 \\ 0 & 0 & dx & dy \end{vmatrix} = 0 \tag{12}$$

Thus the solution:

$$\left(\frac{dy}{dx}\right)^2 - 2tg2\varphi\left(\frac{dy}{dx}\right) - 1 = 0 \quad \Rightarrow \quad \begin{matrix} \left(\frac{dy}{dx}\right)_1 = tg\left(\varphi + \frac{\pi}{4}\right) \\ \left(\frac{dy}{dx}\right)_2 = tg\left(\varphi - \frac{\pi}{4}\right) \end{matrix} \tag{13}$$

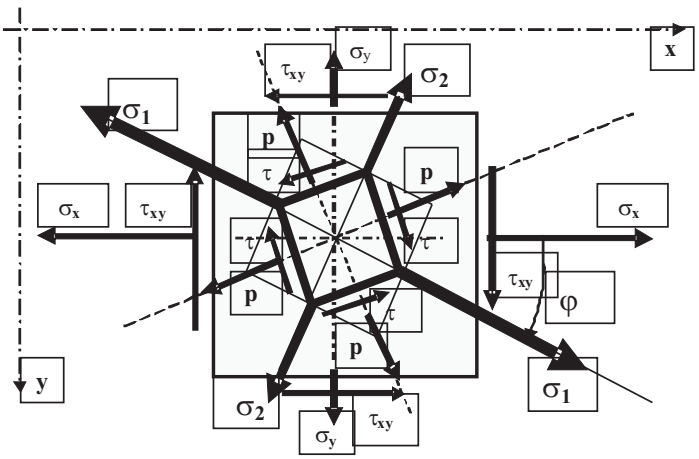

Figure 4 Schematic transformation stresses σ_x, σ_y and τ_{xy} and stresses along the lines of slip $\boldsymbol{p}$ and the principal stressess σ_1, σ_2

We obtain two families of characteristics (13), which form the orthogonal grid and are located at angles relative to the principal stresses certain angle relative to the coordinate system (x, y). Depending on the characteristics satisfied with the alignment sets to zero indicators, which have been introduced or column of free terms of the right sides of equations (11).

After solving the system of equations, two characteristic families (13) are obtained; dependencies fulfilled on characteristics are determined by equating determinants in which columns of free terms - that is, the right sides of the equations of system (11) – have been introduced, to zero.

$$\begin{vmatrix} 1 & 0 & -\frac{1}{2}\left(\frac{\partial m}{\partial x}\cos 2\varphi + \frac{\partial m}{\partial y}\sin 2\varphi\right) & m\cos 2\varphi \\ 0 & 1 & -\frac{1}{2}\left(\frac{\partial m}{\partial x}\sin 2\varphi - \frac{\partial m}{\partial y}\cos 2\varphi\right) & m\sin 2\varphi \\ dx & dy & dp & 0 \\ 0 & 0 & d\varphi & dy \end{vmatrix} = 0$$

$$\Rightarrow dp + md\varphi = -\frac{1}{2}\left(\frac{\partial m}{\partial x}dy - \frac{\partial m}{\partial y}dx\right) \tag{14}$$

$$\begin{vmatrix} -\frac{1}{2}\left(\frac{\partial m}{\partial x}\cos 2\varphi + \frac{\partial m}{\partial y}\sin 2\varphi\right) & 0 & -m\sin 2\varphi & m\cos 2\varphi \\ -\frac{1}{2}\left(\frac{\partial m}{\partial x}\sin 2\varphi + \frac{\partial m}{\partial y}\cos 2\varphi\right) & 1 & m\cos 2\varphi & m\sin 2\varphi \\ dp & dy & 0 & 0 \\ d\varphi & 0 & dx & dy \end{vmatrix} = 0$$

$$\Rightarrow dp - md\varphi = -\frac{1}{2}\left(-\frac{\partial m}{\partial x}dy + \frac{\partial m}{\partial y}dx\right) \tag{15}$$

By solving equations (14) and (15) through substituting the derivatives and differentials with finite differences, a system of equations is obtained, on the basis of which values of the sum of principal stresses p_k, , and the directions of principal stresses φ_k are calculated, followed by the components of the stress state at successive points k.

$$\begin{cases} \left(\frac{dy}{dx}\right)_1 = tg\left(\varphi + \frac{\pi}{4}\right) \\ dp + md\varphi = -\frac{1}{2}\left(\frac{\partial m}{\partial x}dy - \frac{\partial m}{\partial y}dx\right) \end{cases} \tag{16}$$

$$\begin{cases} \left(\frac{dy}{dx}\right)_2 = tg\left(\varphi - \frac{\pi}{4}\right) \\ dp - md\varphi = -\frac{1}{2}\left(-\frac{\partial m}{\partial x}dy + \frac{\partial m}{\partial y}dx\right) \end{cases} \tag{17}$$

$$\begin{cases} tg\left(\varphi_1 + \frac{\pi}{4}\right) = \frac{y_k - y_1}{x_k - x_1} \\ p_k - p_1 + m_1\left(\varphi_k - \varphi_1\right) = w_1 \\ tg\left(\varphi_2 - \frac{\pi}{4}\right) = \frac{y_k - y_2}{x_k - x_2} \\ p_k - p_2 + m_2\left(\varphi_k - \varphi_2\right) = w_2 \end{cases} \tag{18}$$

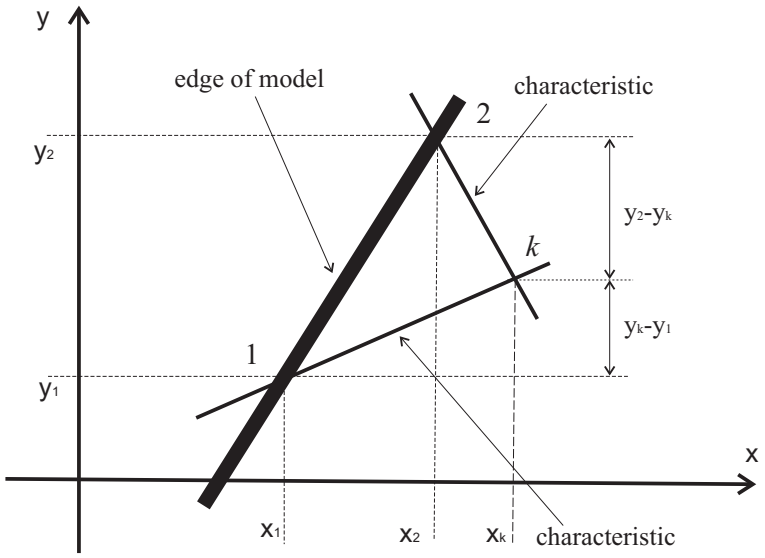

Figure 5 Characteristics

where:

$$\left(\frac{\Delta m}{\Delta y}\right)_1 \cong \frac{m_k - m_1}{y_k - y_1}$$
$$\left(\frac{\Delta m}{\Delta x}\right)_1 \cong \frac{m_k - m_1}{x_k - x_1}$$

and

$$\left(\frac{\Delta m}{\Delta y}\right)_2 \cong \frac{m_k - m_2}{y_k - y_2}$$
$$\left(\frac{\Delta m}{\Delta x}\right)_2 \cong \frac{m_k - m_2}{x_k - x_2}$$

solving the system of equations (18) we get:

$$x_k = \frac{y_2 - y_1 + a_1 x_1 - a_2 x_2}{a_1 - a_2} \qquad y_k = \frac{a_1 a_2 (x_1 - x_2) + a_1 y_2 - a_2 y_1}{a_1 - a_2}$$
$$\varphi_k = \frac{1}{m_1 + m_2}\left[(w_1 - w_2) + (p_1 - p_2) + (m_1\varphi_1 + m_2\varphi_2)\right] \tag{19}$$
$$p_k = \frac{1}{m_1 + m_2}\left[(w_1 m_2 - w_2 m_1) + (p_1 m_2 + p_2 m_1) + m_1 m_2 (\varphi_1 - \varphi_2)\right]$$

The distribution of the stresses (In trems of sum of principal stresses p_k, , and the directions of principal stresses φ_k) were determined from:

$$\sigma_{x_k} = p_k + \frac{m_k}{2}\cos 2\varphi \qquad \sigma_{y_k} = p_k - \frac{m_k}{2}\cos 2\varphi_k \qquad \tau_{xy_k} = \frac{m_k}{2}\sin 2\varphi_k \tag{20}$$

In the case of studies conducted on metal samples, analysis of the stress state using laboratory methods (e.g. the acoustic emission or the photoelastic method as well as optically active coatings, and the caustics method) are laborious and require the use of the appropriate apparatus. For this reason, conducting studies on photoelastic models (made from an optically active material) makes it possible to perform a test in accordance with theoretical assumptions as well as with the standard guidelines, and this makes additional stress analysis over the entire model area possible.

2.3. *Determining material constants*

Properties of the components of experimental model are obtained experimentally. In the case of bending of the model, stresses are equal to:

$$\sigma_x = \sigma_1 = \frac{M_g}{I_z} y \quad \text{and} \quad \sigma_x = \sigma_1 = k_\delta m,$$

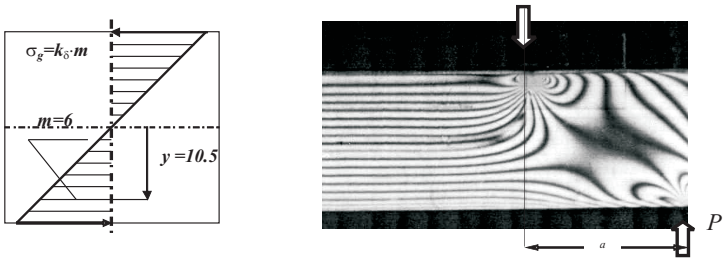

Figure 6 Method of determining the model constant

From this, the value of photoelastic constant of the model is obtained (Fig. 6):

$$k_\delta = \frac{M_g}{I_z} \frac{y}{m} \quad \text{where:} \quad M_y = Pa, \quad I_z = \frac{bh^3}{12}$$

On the basis of experimental studies, the following values were obtained:

- Poisson's ratio ν= 0.36
- photoelastic constant of the model $k_\sigma = 1.74 \div 1.68$ [MPa/fr.] (MPa/order of isochromatic)
- tensile strength $\mathrm{R}_m = 35$ MPa
- compressive strength $\mathrm{R}_c = 120$ MPa
- shear strength $\mathrm{R}_t = 25$ MPa
- Young's modulus E = 3450 MPa.

3. Study of models with fissures

The influence of the presence of non–metallic inclusions, represented as voids, on the distribution of stresses in the sheet was studied. Analysis of the strain process through individual tension stages to the point of destruction inside structures such as the metallographic specimen is practically impossible. That is why photoelastic and numerical models have been developed and made on the basis of metallographic analysis: these models make it possible to study stress and strain inside of the material.

Figure 7 View of the metallographic specimen of the sheet with inclusions

Results of photoelastic studies of models of samples with inclusions have been presented below. Due to the significantly lower values of the strength properties of inclusions in comparison to steel, the inclusions were modeled as voids and narrow fissures. Fissures were created as strips of thin foil removed each time before the conclusion of the resin–hardening process. Models were made from typical EP 52 epoxide resin. Properties and the method of their determination were given in the previous section.

The placement of artificial fissures in the model was similar to the arrangement of actual inclusions observed in views of metallographic specimens of sheets obtained from scrapped overhead crane girders. The studied samples were placed in a polariscope and subjected to uniform tension; isochromatic images were obtained. Changes in the stress state in the area of the inclusion were observed as the load increased.

3.1. *Model with one central fissure*

A single fissure in the center of the sheet thickness is often observed on metallographic specimens of overhead crane sheets. A characteristic image of an inclusion has been presented in Fig. 1, and the manner of cracking of the sample during the tensile test is shown in Fig. 2. It can be seen that the non–metallic inclusion does not exhibit cohesion in the direction transverse to the direction of tension. The assumption can therefore be made that it is modeled as a void.

Fig. 6a shows images of isochromatic lines obtained during stretching of the sample. Studies were conducted in a polariscope under circularly polarized sodium light. The image shows total isochromatic lines (polarizer$\perp$ to analyzer).

Fig. 6b shows an analogous image of partial isochromatic lines in circularly polarized white light (polarizer || to analyzer). Stress concentration is visible near the ends of the fissure. Comparative calculations using the finite element method were also conducted.

3.2. *Models with many fissures*

The images of metallographic specimens show the presence of inclusions as bands irregularly distributed over the surface of the sheet cross–section. Studies of models with inclusions distributed symmetrically relative to the neutral layer were conducted. An exemplary sample is presented on Figs 9 – 12.

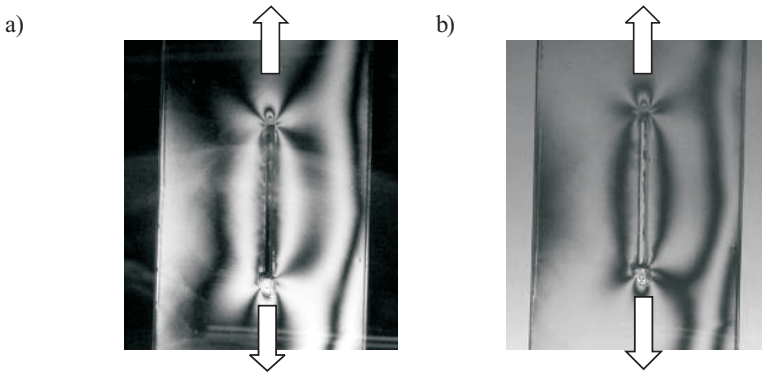

Figure 8 Isochromatic images for the stretched sample with a central fissure: a) Photograph of isochromatic lines insodium light (polarizer $\perp$ to analyzer), b) (polarizer to analyzer)

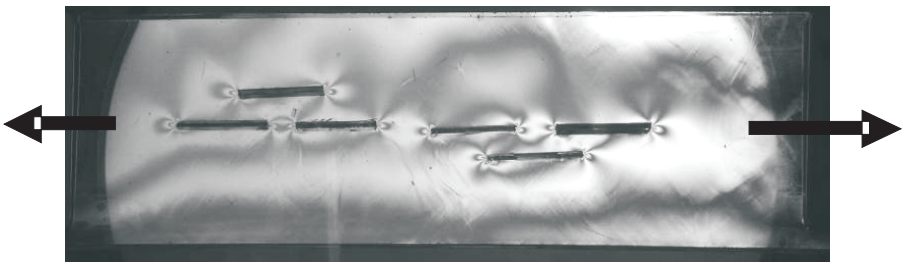

Figure 9 Model with multiple non-metallic inclusions in the initial tension phase. Photograph of isochromatic lines in circularly polarized white light

Photoelastic studies were conducted by increasing the load and analyzing the stress state after each such increase (based on isochromatic line distribution) so as to determine the influence of voids on changes in stress fields and their mutual interaction in the area surrounding voids or fissures. Successive photographs illustrate the course of changes of material effort at increasing loads.

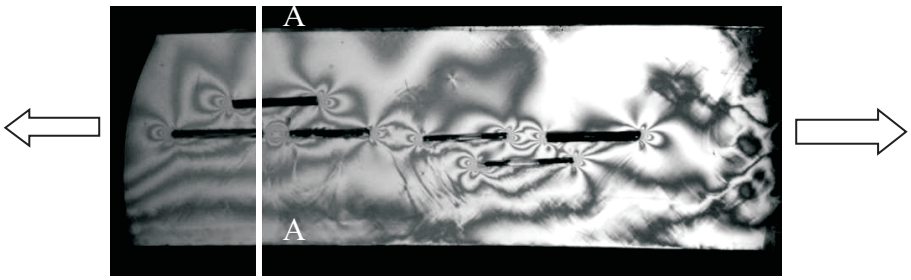

Figure 10 Distribution of isochromatic lines caused by a dislocation of f = 2.4 mm (polarizer ⊥ to analyzer)

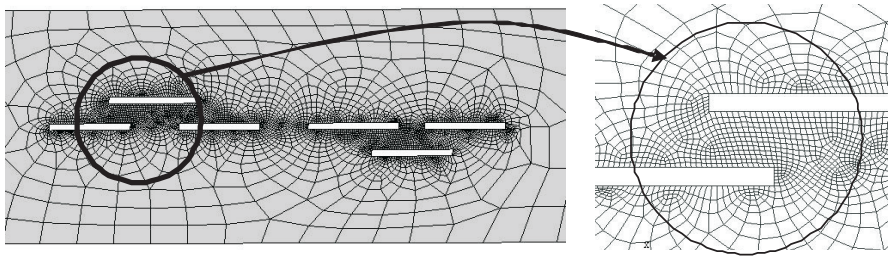

Figure 11 Finite element mesh of the model (used for numerical simulation

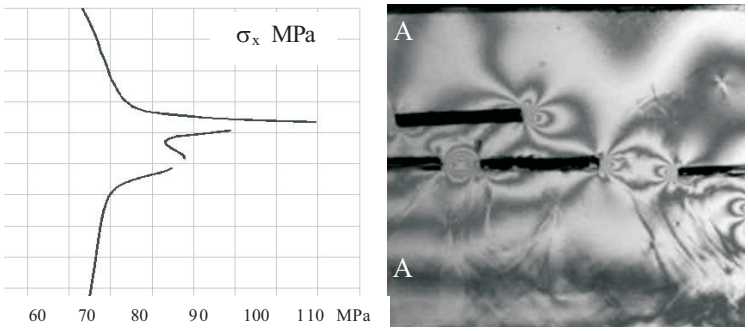

Figure 12 Distribution of stress σ_x obtained experimentally in cross section A-A (in Fig. 10.)

Fig. 10 shows an image of isochromatic lines in the initial loading phase; Fig. 11 and show isochromatic lines for a dislocation of $f = 2.4$ mm, which corresponds to elastic–plastic deformation (=0.02). Studies were conducted under sodium light; total isochromatic lines (polarizer $\perp$ to analyzer) and partial isochromatic lines. Stress concentrations around the vertices of fissures subjected to tension are visible.

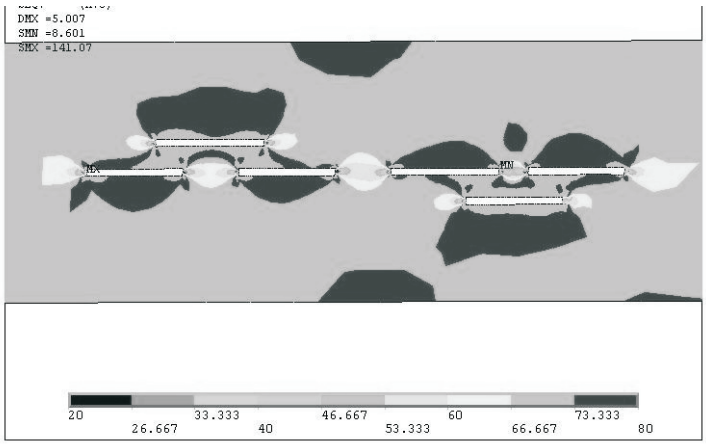

Figure 13 Distribution of reduced stresses according to Huber's hypothesis in the model studied using the photoelastic method obtained by means of the finite element method

4. Numerical Determination of Stress Distribution

The distribution of stresses and displacements has been calculated using the finite element method (FEM) [10, 13]. Based on the images of photoelastic models, analogous numerical models were made and calculations were performed using the finite element method. Calculations were made using two–dimensional models in a coplanar stress state.

Finite element calculations were performed in order to verify the experimentally observed the isochromatic distribution observe the stress state . The geometry and materials of models were chosen to correspond to the actual specimens used in the experiments. The numerical calculations were carried out using the finite element program ANSYS 11 and by applying the substructure technique. A finite element mesh of the model (used for numerical simulation) are presented in Fig. 11.

The numerical (from FEM) isochromatic fringes ($\sigma_1 - \sigma_2$), distribution was shown in Fig.14

5. Results of numerical calculations of the model with fissures simulating lamellar cracks

Comparative calculations using the finite element method were conducted for the same geometrical parameters and the same mechanical properties as the studied models.

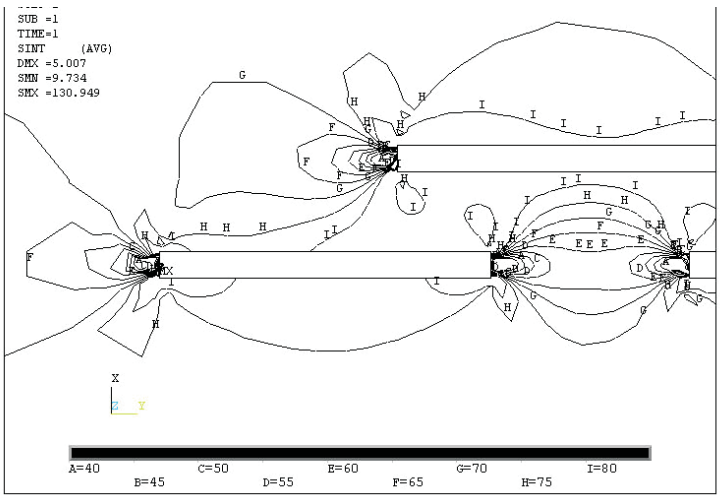

Figure 14 Distribution of of isochromatic in the model using the finite element method

Calculations were made for the same loads as in photoelastic studies, the same material data (that is, material properties), and the same load characteristics.

Stress and strain calculations were conducted for the sample dimensions, material data (that is, material properties), and load characteristics accepted for calculations; the destructive load was determined on the basis of tests.

6. Conclusions

The photoelastic method, as a modeling method for research, is very well suited to analysis of the formation and propagation of lamellar cracks.

This method makes it possible to determine the stress state not only at a specific point, but also to show the entire stress field. It makes it possible to quickly determine points of stress concentration, and thus potential places for formation and propagation of cracks.

The application of the photoelastic method is relatively fast and inexpensive. It is also easy to model inclusions, voids, and possible strengthening of the material (e.g. reinforcement).

This method, like every research method, should be used along with other methods, e.g. experimental and numerical.

It is particularly effective to compare test results with results obtained using the finite element method; this is because, using this method, a numerical image of isochromatic lines can be made, enabling direct comparison of images.

The photoelastic method is very well suited to validation of a numerical model based on the finite element method.

This work has been financed by funds from the National Science Centre.

Project no. 7151/B/T02/2011/40

References

[1] **Doroszkiewicz, R. S.**: Photoelasticity, (in Polish) *PWN*, Warsaw, **1975**.

[2] **Dyląg, Z., Jakubowicz, A. and Orłoś, Z.**: Strength of Materials, (in Polish), *WNT*, Warsaw, **1996**.

[3] **Frocht, M. M.**: Photoelasticity, *John Wiley*, New York, **1960**.

[4] **Blum, A. and Niezgodziski, T.**: Lamellar cracks, *Publisher Institute for Sustainable Technologies – Monographs*, Radom, (in Polish), **2007**.

[5] **Neimitz, A.**: Mechanics of fracture, (in Polish), *PWN*, Warsaw, **1998**.

[6] **Sanford, R. J. and Dally, J. A**: General Method For Determining Mixed–Mode Stress Intensity Factors From Isochromatic Fringe Patterns, *Eng. Fract. Mech.*, Vol. 2, 621–633, **1979**.

[7] **Stupnicki, J.**: Trends of experimental mechanics, *Journ. of Theoterical and Applied Mechanics*, Vol. 2, No 34, 207–233, **1965**.

[8] **Szczepiński W.**: A photoelastic method for determining stresses by means isochromes only, *Archiwes of Applied Mechanics*, 5(13), **1961**.

[9] **Szymczyk, J. and Woźniak, C.**: Continuum modelling of laminates with a slowly graded microstructure, *Archives of Mechanics*, 58, 4–5, 445–458, **2006**.

[10] **User's Guide ANSYS**: 10, 11, Ansys, Inc., Huston, USA, **2009**.

[11] **Woźniak, C.**: Nonlinear Macro–Elastodynamics of Microperiodic Composites, *Bull. Ac. Pol. Sci.: Tech. Sci.*, 41, 315–321, **1993**.

[12] **Woźniak, C.**: Microdynamics: Continuum.Modelling the Simple Composite Materials, *J. Theor. Appl. Meeh.*, 33, 267–289, **1995**.

[13] **Zienkiewicz, O. C.**: The Finite Element Method in Engineering Science, *Mc Graw – Hill*, London, New York, **1971**.